Journal of Sound and Vibration (1997) **201**(2), 169–187

IMPEDANCE-BASED MODELLING OF INDUCED STRAIN ACTUATORS BONDED ON RING STRUCTURES

F. Lalande, Z. Chaudhry and C. A. Rogers

Center for Intelligent Material Systems and Structures, Virginia Polytechnic Institute and State University, Blacksburg, VA 24061-0261, *U.S.A.*

(*Received* 10 *July* 1995, *and in final form* 30 *August* 1996)

An impedance-based model to describe the in-phase, out-of-phase and unsymmetric actuation of induced strain actuators bonded to the surface of a circular ring has been developed. The essence of the impedance approach is to match the actuator impedance with the structural impedance at the ends of the actuators, which includes the dynamic effects of the system. In the model derivation, the dynamics of the ring are based on the Rayleigh–Ritz method. The appropriate representation of the loading due to induced strain actuation is discussed. The in-phase and out-of-phase actuation authority is compared. It is shown that out-of-phase actuation has higher authority in exciting the lower order bending modes, while in-phase actuation has higher authority in exciting the higher order circumferential modes. In-phase actuation does excite the lower order bending modes through the in-plane and out-of-plane displacement coupling, but with an order of magnitude lower than out-of-phase actuation. A good correlation between the dynamic finite element analysis using piezoelectric elements available in ANSYS 5.0 is found. Experimental results of a circular ring actuated in-phase and out-of-phase are also presented. Different methods of bonding straight actuators on curved surfaces are investigated. Experimental verification of the impedance-based models is conclusive, particularly for the out-of-phase actuation.

1. INTRODUCTION

Structural vibration control has always been important in the design of efficient and reliable mechanical systems. Recently, a novel approach using induced strain actuators for such vibrational control has been presented, which can also be extended to acoustic control. Induced strain actuators are particularly interesting because they can be fully integrated in or on the structure itself. By applying forces directly on the structure at critical locations, efficient structural control can be obtained. In vibrational and acoustic control, the undesirable dynamic effects are eliminated by modifying the apparent structural impedance through the induced strain actuators. This approach eliminates the moving parts encountered in the bulky shaker-type actuators which are conventionally used. Such actuators, since they are bonded right on the surface of the structure, do not need a back reaction to function.

When induced strain actuator patches, such as piezoelectrics, are symmetrically bonded to the surface on each side of the structure, they generate a set of forces along the edges of the actuators. The two actuators can be activated in-phase or out-of-phase. In-phase actuation refers to the case in which both actuators expand and contract together. This type of actuation creates extensional in-plane forces on the structure. Out-of-phase

0022–460X/97/120169 + 19 $25.00/0/SV960764

actuation refers to the case in which one actuator expands and the other contracts, and *vice versa*. Bending moments distributed along the edges of the actuator patch are applied to the structure when out-of-phase actuation is used. Thus, depending upon the type of actuation used, the same actuator set-up can generate a very different structural actuation and response.

Theoretical studies based on the static application of piezoelectric forces and moments on beam structures have been proposed [1–4]. Models have also been extended to two-dimensional plate structures [5, 6], and adaptations of plate models to shells structures have been proposed [7, 8]. Models based on shell equations have also been proposed [9–11].

Theoretical impedance-based models that include the dynamic interaction between the actuators and the structure have also been proposed for beams [12], plates [13] and shells [14, 15]. The essence of the impedance approach is to match the actuator impedance to the structural impedance at the edges of the actuators. The impedance models are more accurate in the modelling of the structural response. Most of the models mentioned have been developed for pure out-of-phase loading, except for the in-phase model presented by Lester and Lefebvre [7].

All of the theoretical models referred to above were developed independently, without any comparison of the authority of in-phase and out-of-phase actuation. Only Lester and Lefebvre [7] performed such a comparison and some drawbacks are presented in the modelling. No self-equilibrium considerations for the in-phase actuation were included, and the shell model is a simple plate adaptation. It has been shown that special considerations need to be made to eliminate the rigid body transverse forces inherent in curved structures when in-phase actuation is used [16]. The action of the actuators has to be represented by an equivalent in-plane force and a transverse pressure applied in the region of the actuator patch.

The previously developed impedance models for shell structures have some weaknesses. Zhou *et al*. [15] modelled the out-of-phase actuation of a circular cylinder with a discrete line moment applied along the edges of the actuator in which the transverse shear stress was neglected as a simplification. Rossi *et al*. [14] studied the out-of-phase actuation of a circular ring using a uniform induced moment on the actuator footprint, in which the structural mechanical impedance definition was not appropriate: the mechanical impedance was defined as the tangential force divided by the tangential velocity at the end of the actuator bonded on the top surface of the ring only. This definition would be appropriate if a single actuator were bonded to the ring on the top surface. For out-of-phase actuation, the ring is subjected to a pure moment generated by forces applied on the ring by actuators bonded on the top and bottom surfaces of the ring. Since the forces are coupled, the force applied on the ring by the actuator on the bottom surface should also be included, since it will have an impact on the displacements on the top surface of the ring, and *vice versa*. Thus, the proper definition of the impedance based on the tangential force and the tangential velocity at the end of the actuator should be as follows:

$$\begin{Bmatrix} F_{top} \\ F_{bottom} \end{Bmatrix} = \begin{bmatrix} Z_{tt} & Z_{bt} \\ Z_{tb} & Z_{bb} \end{bmatrix} \begin{Bmatrix} \dot{v}_{top} \\ \dot{v}_{bottom} \end{Bmatrix}. \tag{1}$$

This equation can be simplified by substituting $F_{top} = -F_{bottom} = F$ for out-of-phase actuation. Also, the mechanical impedance can be defined as the moment divided by the rotational velocity at the ends of the actuator, as in Zhou *et al*. [14]. This latter approach will be used for its accuracy as well as its simplicity. Both impedance definitions can be shown to be equal through simple geometrical relations.

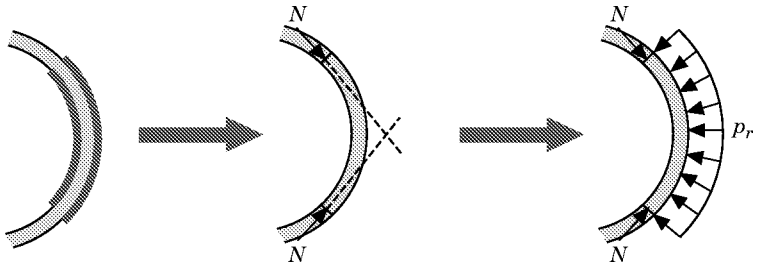

Figure 1. The in-phase equivalent loading to maintain self-equilibrium of the shell structure.

In this paper, a discussion of the appropriate representation of the equivalent induced strain loading for rings is first presented. Then, an impedance-based model of a circular ring actuated in-phase, out-of-phase and unsymmetrically is derived. The Rayleigh–Ritz method is used to model the structural dynamic characteristics. A comparison of the authority of in-phase and out-of-phase actuation is presented. This is followed by a theoretical case study and a finite element analysis. Also, an experimental verification of the impedance models for both in-phase and out-of-phase actuation is presented.

2. INDUCED STRAIN EQUIVALENT LOADING

In a recent paper, Chaudhry *et al*. [16] considered the modelling of piezoelectric actuator patches bonded on the surface of circular cylinders. When the piezoelectric actuators are actuated in phase, it was found that the point force model used to represent the actuator creates a rigid body motion, since the equivalent line forces are not collinear due to the curvature of the ring (see Figure 1). Since the PZT actuators are integrated within the structure, self-equilibrium must be satisfied. Also, when the piezoelectric actuators are actuated out of phase, the loading coming from the shear stress resultant is often neglected compared to the tangential stress resultant.

To eliminate this non-equilibrium state of the ring, a transverse uniform pressure is added (see Figure 2) to the in-phase actuation loading and the shear stress resultant is added to out-of-phase actuation loading. This self-equilibrating equivalent loading is included in the ring governing equations as external loading. The magnitude of the transverse pressure from simple statics is then

$$p_r = -N/R, \tag{2}$$

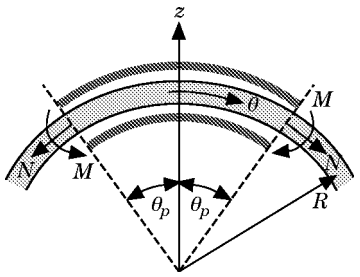

Figure 2. A one-dimensional ring with bonded PZT actuators in-phase, out-of-phase and unsymmetric. The force applied by the actuators at the edge is shown.

where the static force and moment magnitudes are

$$N = \frac{2Y_s t_s}{2+\psi}\Lambda, \qquad M = Y_s t_s \frac{t_s + t_a}{6+\psi}\Lambda, \tag{3a, b}$$

with

$$\psi = Y_s t_s / Y_a t_a, \tag{4}$$

where Y, t, Λ and R are the Young's modulus, the thickness, the free induced strain and the radius of the ring, respectively, while the subscripts s and a denote the shell and actuator, respectively. Another approach to maintaining equilibrium is to include induced strain actuation as induced uniform loading on the actuator footprint. A comparison between the external loading and the induced uniform loading will now be presented.

Using the thin ring theory of a circular ring [17], the equations of motion can be written in terms of the internal membrane force, $N_{\theta\theta}$, with the actuator-induced uniform tangential force, n, and in terms of the internal bending moment $M_{\theta\theta}$, with the actuator induced-uniform moment m:

$$\frac{\partial(N_{\theta\theta} - n)}{R\,\partial\theta} + \frac{\partial(M_{\theta\theta} - m)}{R^2\,\partial\theta} = \rho_s t_s \ddot{v}^o, \qquad \frac{\partial^2(M_{\theta\theta} - m)}{(R\,\partial\theta)^2} - \frac{(N_{\theta\theta} - n)}{R} = \rho_s t_s \ddot{w}^o, \tag{5a, b}$$

where the discrete induced uniform tangential and axial forces and moments can be written using Heaviside functions:

$$n = N[\mathrm{H}(\theta - \theta_1) - \mathrm{H}(\theta - \theta_2)], \qquad m = M[\mathrm{H}(\theta - \theta_1) - \mathrm{H}(\theta - \theta_2)]. \tag{6a, b}$$

The actuator-induced uniform tangential and axial forces and moments can be transferred to the right side of the equation:

$$\frac{\partial N_{\theta\theta}}{R\,\partial\theta} + \frac{\partial M_{\theta\theta}}{R^2\,\partial\theta} = \rho_s t_s \ddot{v}^o + \frac{\partial n}{R\,\partial\theta} + \frac{\partial m}{R^2\,\partial\theta}, \tag{7a}$$

$$\frac{\partial^2 M_{\theta\theta}}{(R\,\partial\theta)^2} - \frac{N_{\theta\theta}}{R} = \rho_s t_s \ddot{w}^o - \frac{n}{R} + \frac{\partial^2 m}{(R\,\partial\theta)^2}. \tag{7b}$$

Similarly, for external loading, the ring governing equations can be written in terms of the equivalent external loading, the tangential line force and moment, n^* and m^*, and the uniform radial pressure, p_r^* [17]:

$$\frac{\partial N_{\theta\theta}}{R\,\partial\theta} + \frac{\partial M_{\theta\theta}}{R^2\,\partial\theta} = \rho_s t_s \ddot{v}^o + \frac{n^*}{R} + \frac{m^*}{R^2}, \tag{8a}$$

$$\frac{\partial^2 M_{\theta\theta}}{(R\,\partial\theta)^2} - \frac{\partial N_{\theta\theta}}{R} = \rho_s t_s \ddot{w}^o + p_r^* + \frac{\partial m^*}{R^2\,\partial\theta}, \tag{8b}$$

where the external equivalent loading can be written using Dirac delta functions:

$$n^* = N[\delta(\theta - \theta_1) - \delta(\theta - \theta_2)], \qquad p_r^* = -\frac{N}{R}[\mathrm{H}(\theta - \theta_1) - \mathrm{H}(\theta - \theta_2)], \tag{9a, b}$$

$$m^* = M[\delta(\theta - \theta_1) - \delta(\theta - \theta_2)]. \tag{9c}$$

From equations (6–9), it can be seen that whether actuator-induced uniform loading or external equivalent loading are used, the equations of motion are the same. Thus, the tangential force and moment produced by the actuators can be included in the governing equations either as induced uniform loading on the actuators' footprint or as external equivalent loading on the actuators' edges.

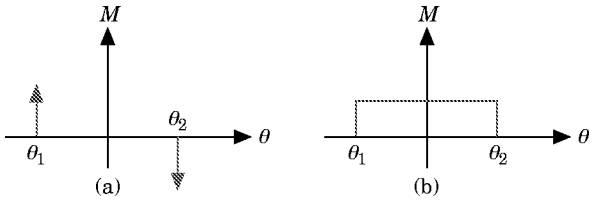

Figure 3. Different representations of the induced strain actuation loading: (a) external equivalent loading $m^* = M[\delta(\theta - \theta_1) - \delta(\theta - \theta_2)]$; (b) induced uniform loading $m = M[H(\theta - \theta_1) - H(\theta - \theta_2)]$.

The external equivalent loading can be seen as the pin-force approach, since the actuator is simply replaced by line force and moment of appropriate magnitude on the actuator edges using Dirac delta functions (Figure 3(a)) along with a uniform pressure to maintain self-equilibrium for in-phase actuation. The induced uniform loadings are not considered to be external and are included in the equilibrium equations in a similar fashion to thermal loading. The induced forces and moments are considered uniform over the actuator footprint and are represented using Heaviside functions (Figure 3(b)).

3. ACTUATOR RESPONSE SUPERPOSITION

The superposition of the response due to a single actuator to obtain a pure in-phase or out-of-phase response is now considered [18]. If the displacements due to the inside actuator are subtracted from the displacements due to the outside actuator, the pure out-of-phase solution is obtained exactly (equation (10a)). If the displacements are added, the pure in-phase solution is also obtained exactly (equation (10b)):

$$u_i|_{Outside} - u_i|_{Inside} = u_i|_{Outphase}, \qquad u_i|_{Outside} + u_i|_{Inside} = u_i|_{Inphase}. \tag{10a, b}$$

The converse is also true. The structural response of a single actuator bonded on the inside or outside surface of the shell can be obtained from the in-phase and out-of-phase structural responses (equation (11)):

$$\tfrac{1}{2}u_i|_{Inphase} + \tfrac{1}{2}u_i|_{Outphase} = u_i|_{Outside}, \qquad \tfrac{1}{2}u_i|_{Inphase} - \tfrac{1}{2}u_i|_{Outphase} = u_i|_{Inside}. \tag{11a, b}$$

Any unsymmetrical voltage application on the actuators can be expressed as a linear combination of pure in-phase loading and pure out-of-phase loading. The appropriate weighting factors for in-phase (ξ^i) and out-of-phase actuation (ξ^o), which are based on the free induced strains (Λ) applied on each actuators, are

$$\xi^i = \frac{\Lambda_{inside} + \Lambda_{outside}}{2\Lambda_{max}}, \qquad \xi^o = \frac{-\Lambda_{inside} + \Lambda_{outside}}{2\Lambda_{max}}, \tag{12a, b}$$

where Λ_{max} is the absolute value of the largest actuator free induced strain (inside or outside). On the basis of this definition, the free induced strain ratios ξ^i and ξ^o will vary from $-1/2$ to 1, $\xi^o = 1$ being pure out-of-phase and $\xi^i = 1$ being pure in-phase. The ξ ratios are dependent only on the free induced strain, assuming that identical actuators are bonded on both sides of the shell. For cases in which the actuators do not have the same thicknesses, the equation derivation becomes more complicated due to different actuator impedances. However, a simple superposition of the structural response to actuators bonded on the inside and on the outside of the shell can still be used to predict the dynamic response using this method.

4. IMPEDANCE MODEL DERIVATION

An impedance model of a free floating thin circular ring excited by a pair of PZT actuators is presented (see Figure 2). The impedance model is derived in four major steps: (1) calculation of the structural impedance at the edges of the actuators using the ring governing equations and appropriate boundary conditions; (2) calculation of the actuator impedance; (3) calculation of the actuator output force based on the structural and actuator impedances interaction; and (4) application of the frequency dependent actuator output force to the ring governing equations to obtain the ring response. The PZT patches are assumed to be perfectly bonded to the structure, so that the action of the PZT actuators can be replaced by discrete line forces along the edges of the actuators. The linear Love–Kirchhoff theory [19, 20] is used since the ring is assumed to be thin and the stress distribution through the thickness of the actuators is assumed to be constant. The symmetry of the system will be considered in the development of the impedance model.

4.1. DETERMINATION OF THE STRUCTURAL IMPEDANCE

The structural impedance is defined on the basis of discrete applied loads and velocities at the ends of the actuators. For in-phase actuation, the mechanical admittance, H_{in}, is defined on the basis of the tangential velocity, $\dot{v}$ (equation (13a)) while for out-of-phase actuation, H_{out}, it is defined on the basis of rotational velocity, $\dot{\theta}$ (equation (13b)):

$$H_{in} = -\dot{v}/N, \qquad H_{out} = -\dot{\theta}/M, \tag{13a, b}$$

where the minus sign in the previous equations is necessary to take account of the opposite or negative reactions of the structure to the output forces of the actuators. The mechanical impedance, Z, is simply the inverse of the mechanical admittance, H. The discrete applied in-phase tangential force and out-of-phase moment on the structure are (see Figure 2)

$$N = 2F\xi^i, \qquad M = (t_a + t_s)F\xi^o, \tag{14a, b}$$

where F is the actuator output force.

The impedance calculation at the ends of the actuator can be carried out using the Rayleigh–Ritz technique. The equation of motion for the ring can be written in matrix form (equation (7)) as [1]

$$\begin{Bmatrix} K\left[\frac{\partial^2}{R^2\,\partial\theta^2}\right] + \frac{D}{R^2}\left[\frac{\partial^2}{R^2\,\partial\theta^2}\right] & \frac{K}{R}\left[\frac{\partial}{R\,\partial\theta}\right] - \frac{D}{R}\left[\frac{\partial^3}{R^3\,\partial\theta^3}\right] \\ -\frac{K}{R}\left[\frac{\partial}{R\,\partial\theta}\right] + \frac{D}{R}\left[\frac{\partial^3}{R^3\,\partial\theta^3}\right] & -\frac{K}{R^2} - D\left[\frac{\partial^4}{R^4\,\partial\theta^4}\right] \end{Bmatrix} \begin{Bmatrix} v^o \\ w^o \end{Bmatrix} - \rho_s t_s \begin{Bmatrix} \ddot{v}^o \\ \ddot{w}^o \end{Bmatrix}$$

$$= \begin{Bmatrix} \frac{\partial m_\theta}{R^2\,\partial\theta} + \frac{\partial n_\theta}{R\,\partial\theta} \\ \frac{1}{R}\left(\frac{\partial^2 m_\theta}{R\,\partial\theta^2}\right) - \frac{n_\theta}{R} \end{Bmatrix}, \tag{15}$$

where the bending and extensional stiffnesses are

$$D = Y_s t_s^3/12, \qquad K = Y_s t_s, \tag{16a, b}$$

respectively, Y_s is the complex Young's modulus of the ring, and ρ_s is the density of the ring. The complex Young's modulus is used to include the damping through the structural damping factor. The Poisson ratio is not present in the stiffness expressions due to the one-dimensional state of the ring. Taking into consideration the free floating boundary conditions of the ring, the tangential and radial neutral axes displacements, v^o and w^o, respectively, have the following assumed solutions [21]:

$$v^o(t, \theta) = \sum_{n=0}^{\infty} V_n \sin(n\theta)\, e^{i\omega t}, \qquad w^o(t, \theta) = \sum_{n=0}^{\infty} W_n \cos(n\theta)\, e^{i\omega t}. \tag{17a, b}$$

Introducing the tangential and radial displacement expressions (17) in the equation of motion (15), a linear system of equations is obtained:

$$\begin{bmatrix} -\dfrac{D}{R^4}n^2 - \dfrac{K}{R^2}n^2 + \rho_s t_s \omega^2 & -\dfrac{D}{R^4}n^3 - \dfrac{K}{R^2}n \\ -\dfrac{D}{R^4}n^3 - \dfrac{K}{R^2}n & -\dfrac{D}{R^4}n^4 - \dfrac{K}{R^2} + \rho_s t_s \omega^2 \end{bmatrix} \begin{Bmatrix} V_n \\ W_n \end{Bmatrix} = \begin{Bmatrix} \dfrac{M}{R} + N \\ \dfrac{Mn}{R} + \dfrac{N}{n} \end{Bmatrix} \frac{\sin(n\theta_p)}{\pi R}, \tag{18a}$$

and, for $n = 0$,

$$\begin{bmatrix} \rho_s t_s \omega^2 & 0 \\ 0 & -\dfrac{K}{R^2} + \rho_s t_s \omega^2 \end{bmatrix} \begin{Bmatrix} V_0 \\ W_0 \end{Bmatrix} = \begin{Bmatrix} 0 \\ -\dfrac{N\theta_p}{2\pi R} \end{Bmatrix}. \tag{18b}$$

Making use of linear superposition, the admittance for unsymmetric loading can be separated into two parts, representing pure in-phase actuation admittance and pure out-of-phase actuation admittance:

$$H_{in} = \frac{2i\omega}{\pi R}\, \xi^i \sum_{n=1}^{\infty} \left\{ \frac{[\rho_s t_s \omega^2 + (D/R^4)n^2(1 - n^2)] \sin^2(n\theta_p)}{(DK/R^6)(n^2 - 1)^2 - (n^2 + 1)(Dn^2/R^4 + K/R^2)\rho_s t_s \omega^2 + (\rho_s t_s \omega^2)^2} \right\}, \tag{19a}$$

$$H_{out} = \frac{2i\omega}{\pi R^3}\, \xi^o \sum_{n=1}^{\infty} \left\{ \frac{[(Kn^2/R^2)(1 - n^2) + \rho_s t_s \omega^2] \sin^2(n\theta_p)}{(DK/R^6)(n^2 - 1)^2 - (n^2 + 1)(Dn^2/R^4 + K/R^2)\rho_s t_s \omega^2 + (\rho_s t_s \omega^2)^2} \right\}. \tag{19b}$$

4.2. DETERMINATION OF THE ACTUATOR IMPEDANCE

With the structural impedance now determined, the next step in the impedance approach is to calculate the actuator impedance. The actuators bonded on the ring are excited by applying an electric field in the radial polarization direction. Under Love's assumptions for thin rings, the equation of motion of a ring vibrating in the tangential direction can be expressed as

$$\rho_a \ddot{v}^o(t, \theta) = Y_a^E\, \partial \varepsilon_\theta / R\, \partial \theta, \tag{20}$$

where ρ_a is the PZT density and Y_a^E is the PZT complex Young's modulus at zero electric field, such that the mechanical dissipation of the actuator can be included.

The piezoelectric actuator patch is thin and has a large radius of curvature with a limited length in the tangential direction. In other words, the actuator's patches are almost flat. These characteristics enable us to simplify the problem by assuming the actuators to be flat, and the strain–displacement relation is given by equation (21). As a practical matter,

for practical cases, the bending of the flat PZT actuator patches on the structure is very limited due to the brittle nature of piezoelectric material:

$$\varepsilon_\theta = \partial v^o(t, \theta)/R\,\partial\theta. \tag{21}$$

Thus, the equation of motion in the tangential direction will be used:

$$\rho_a \ddot{v}^o(t, \theta) = Y_a^E\,\partial^2 v^o(t, \theta)/R^2\,\partial\theta^2. \tag{22}$$

Solving equation (22) and assuming harmonic excitation by separating the displacement into time and spatial domain, the tangential displacement response of the actuator is given by

$$v^o(t, \theta) = [A\,\sin kR\theta + B\,\cos kR\theta]\,\mathrm{e}^{\mathrm{i}\omega t}, \tag{23}$$

where ω is the input angular velocity, and the wavenumber is given by

$$k^2 = \omega^2(\rho_a/Y_a^E). \tag{24}$$

The short-circuit input impedance of the piezoelectric actuator is defined as [12]

$$Z_a = Y_a^E t_a k/\mathrm{i}\omega\,\tan kR\theta_p. \tag{25}$$

The constitutive equation of the piezoelectric actuator is

$$\varepsilon_\theta = \partial v^o/R\,\partial\theta = F/Y_a^E t_a + d_{32}E, \tag{26}$$

with d_{32} and E being the piezoelectric constant of the actuators and the electric field applied to the actuators, respectively.

4.3. STRUCTURE/ACTUATOR DYNAMIC INTERACTION

In this section, the dynamic interaction between the actuators and the ring structure is under study. The essence of impedance modelling is to match the structural impedance with the actuator's impedance at its ends; the dynamic actuator force output is thus obtained.

Using the constitutive equations of the PZT actuator (equation (26)) and applying the proper boundary conditions [14, 15], the actuator force output of the actuator at θ_p is given by

$$F = -Z|_{\theta_p} d_{32} E t_a\, Y_a^E/(Z|_{\theta_p} + Z_a), \tag{27}$$

At this point, the dynamic actuator force output has been calculated based on the structural and actuator impedances.

4.4. RING RESPONSE CALCULATIONS

Using the dynamic actuator force output, the ring response can be calculated on the basis of the ring governing equation developed in section 4.1. The tangential and radial displacements are given in equation (17).

5. THEORETICAL RESULTS

The impedance model is applied to a case study of a circular steel ring with G1195 piezoelectric actuator patches. The theoretical results will be limited to in-phase and out-of-phase actuation. The material and geometric properties of the system are shown in Table 1. The size of the PZT actuator was kept small enough (10°) to satisfy the impedance model assumptions. The results from the static approach are compared to those from the impedance model. A comparison between the in-phase and out-of-phase

TABLE 1

Material and geometric properties of the PZT actuator and the steel ring

	Steel ring	PZT actuator
Young's modulus (Pa)	$190{\cdot}5 \times 10^9$	63×10^9
Density (kg/m^3)	7850	7650
Loss factor	0·006	0·001
Piezoelectric coefficient, d_{32} (m/V)	N/A	-166×10^{-12}
Applied electric field (V/m)	N/A	$6{\cdot}0 \times 10^5$
Radius/length (cm)	30·16	3·76
Width (cm)	3·175	3·175
Thickness (mm)	6·3	0·25

actuation of a ring structure is also performed. The comparison focuses on the structural radial displacements produced by the actuators and on the efficiency to excite the structural resonant modes. These are the most relevant factors needed when vibration and noise control is considered.

In Figure 4 are shown the structural impedances for both in-phase and out-of-phase actuation. The in-phase impedance, for the case being considered, has a greater magnitude than the out-of-phase impedance. For comparison, the actuator impedance (the dashed curve) is also shown in Figure 4. Good actuation authority is obtained when the structural and actuator impedances are of the same order of magnitude [15]. On the basis of this observation, in-phase actuation will have limited authority on the structure compared to out-of-phase actuation. If a thicker actuator is used, the actuator impedance is increased and the dynamic interaction between the actuator and the structure is increased. However, for in-phase actuation, an unreasonable thickness is needed to obtain a good interaction. The first six bending modes, which are the lower peaks, are shown in Figure 4. Out-of-phase actuation has a larger impact on the structure at resonant frequencies as

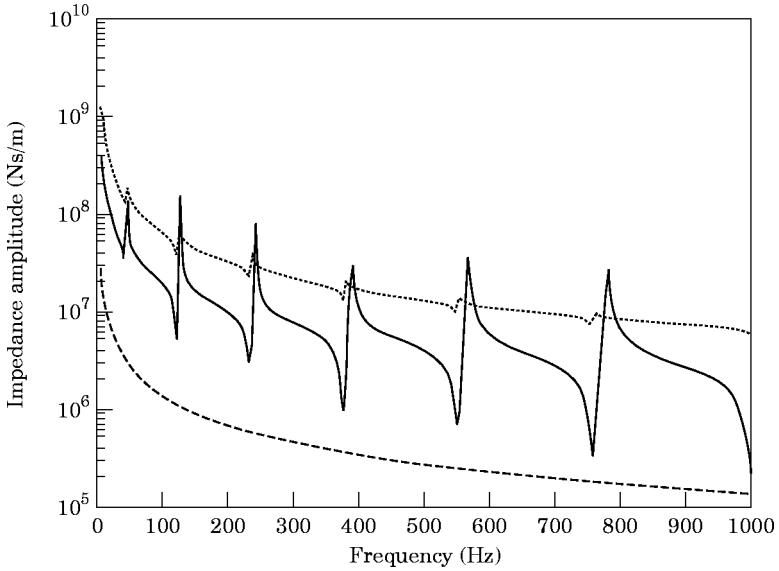

Figure 4. The structural impedance for in-phase and out-of-phase actuation. ——, Out-of-phase actuation; · · · ·, in-phase actuation; ----, actuator impedance.

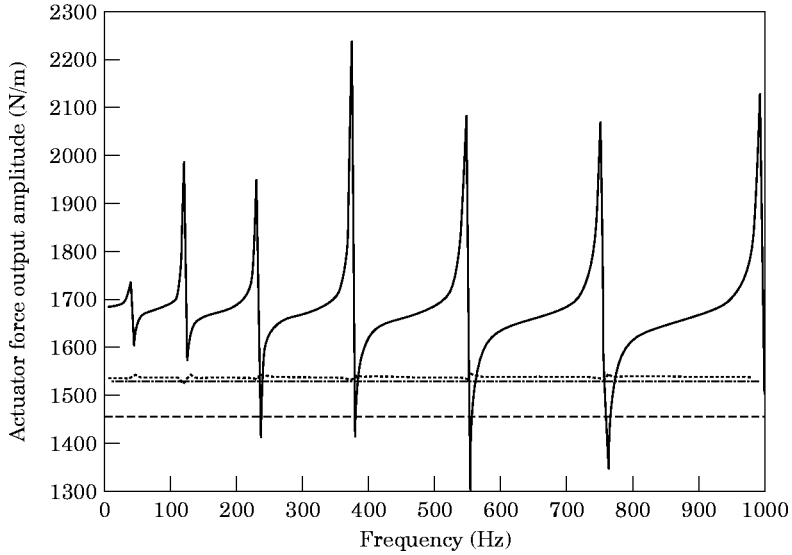

Figure 5. Actuator output forces for in-phase and out-of-phase actuation based on impedance and static model. Out-of-phase: ——, impedance model; ----, static model. In-phase: · · · · , impedance model; -·-·-·, static model.

compared to in-phase actuation. Indeed, when the ring is actuated in phase, the bending modes are only slightly excited through the in-plane/out-of-plane coupling property of shells. However, as opposed to out-of-phase actuation, the in-phase actuation has the capability of exciting the higher frequency circumferential modes.

In Figure 5 is shown the actuator output force for in-phase and out-of-phase actuation. The dotted horizontal line is the actuator force output calculated with the static approach [2]. It can be observed that the actuator force output is heavily dependent on the excitation frequency in the case of out-of-phase actuation, which is not the case for in-phase actuation. It can be concluded that the first natural modes, which are bending modes, are only slightly excited by the in-phase actuation of the ring. The difference in the force magnitude between impedance and the static model is less than 1% at $\omega = 0$.

The radial displacement frequency response at 30° from the actuator is presented in Figure 6. The displacements produced by in-phase actuation are an order of magnitude smaller than those obtained by out-of-phase actuation, for the same electrical field applied to the piezoelectric actuators. Unlike in-phase actuation, out-of-phase actuation is very effective in exciting the natural bending modes of the structure. Since the frequency range of interest in structural vibration control is low, out-of-phase actuation is thus more efficient than in-phase actuation for ring structures. The dotted lines are from the finite element analysis, which will be discussed in the next section.

Based on an impedance model developed for two-dimensional shells (by Lalande *et al*. [18]), the response of a shell of the same dimension as the ring (Table 1) but 75 cm long has been calculated. The actuator center is at co-ordinates $x = 37{\cdot}5$ cm, $\theta = 0°$. The radial displacement frequency response at $x = 15$ cm, $\theta = 30°$ is presented in Figure 7. Once again, the displacements produced by in-phase actuation are smaller than those produced by out-of-phase actuation. However, the clear advantage of using out-of-phase over in-phase that was found for one-dimensional rings is not as obvious for two-dimensional shells.

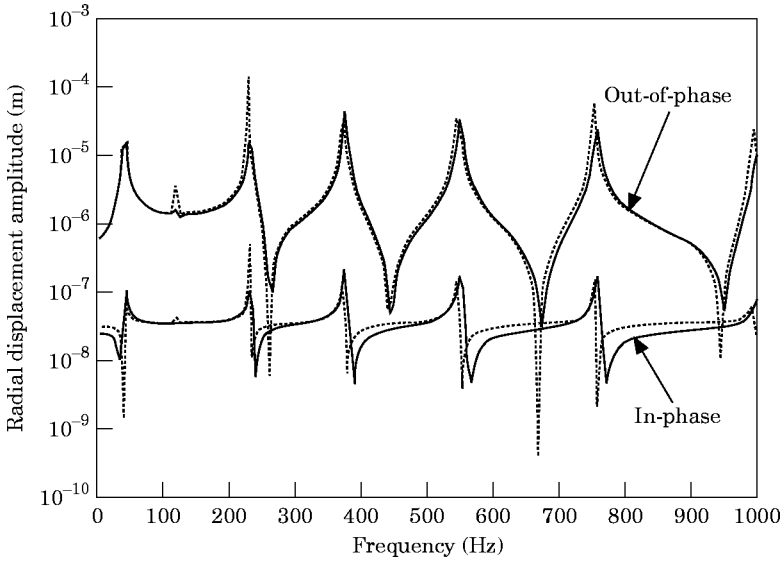

Figure 6. An authority comparison of in-phase and out-of-phase actuation for a one-dimensional ring. ——, Impedance model; · · · ·, finite element analysis.

This conclusion is different from that reported by Lester and Lefebvre [7]. In their paper, a theoretical model based on a static approach was presented for in-phase and out-of-phase actuation of cylinders. It is stated that in-phase actuation excites the lower bending modes more efficiently than out-of-phase actuation. The reason for this erroneous conclusion is simply the omission of the self-equilibrating pressure that needs to be used for in-phase actuation. Without the pressure loading, the shell response will produce erroneous larger displacements.

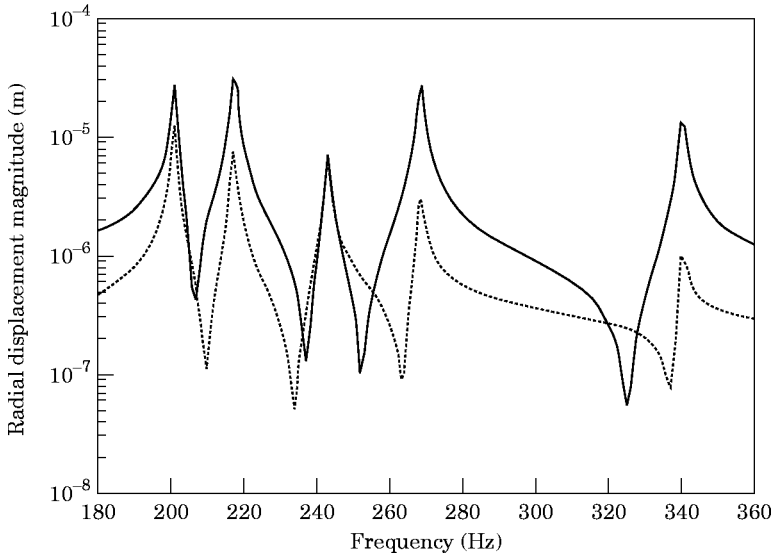

Figure 7. An authority comparison of in-phase and out-of-phase actuation for a two-dimensional shell. ——, Out-of-phase actuation; · · · ·, in-phase actuation.

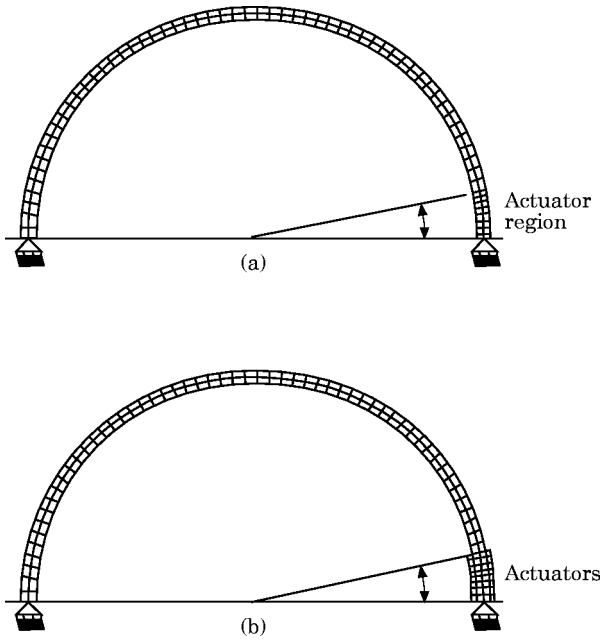

Figure 8. The finite element model (a) without and (b) with actuators.

6. FINITE ELEMENT ANALYSIS

The finite element technique has been used and compared to the theoretical impedance model. The dynamic analysis was performed using piezoelectric elements available in ANSYS 5·0. An harmonic electrical field was applied to the piezoelectric elements in two finite element models. The first model does not include the actuators that are bonded to the surface of the ring. Instead, the structure itself in the region of the actuator is modelled with the piezoelectric elements, to which the harmonic electrical field is applied (Figure 8(a)). The second model includes the piezoelectric actuators on the structure, to which the electrical field is applied (Figure 8(b)). The theoretical results are expected to match the finite element model without the actuators' since the stiffness and mass added by the actuators is not considered in the structural response calculations. The finite element results, including the actuator mass and stiffness, should be close to the theoretical predictions due to the small thickness and size of the actuators. For both finite element models, the symmetry of the structure was used to reduce the size of the models. The structure was modelled using plane stress elements and the actuators (with the actuator model) or actuator region (without the actuator model) were modelled using piezoelectric plane stress elements. Free floating boundary conditions have been used for both models. In the modelling of the piezoelectric elements, great care must be taken in the input of the piezoelectric material properties to obtain accurate results.

The frequency response of the ring using finite elements at 30° from the actuators is shown in Figure 6, along with the impedance models' frequency responses. The frequency response of the impedance model matches the dynamic finite element analysis with great accuracy. The finite element natural frequencies are a little lower than those obtained from the impedance models, due to the increased stiffness provided by the actuators in the finite element model. With an increasing actuator size, this discrepancy increases too.

The next step is to look at the structural response at low frequency (5 Hz), where the response of the ring will be similar to the static response. The radial displacement

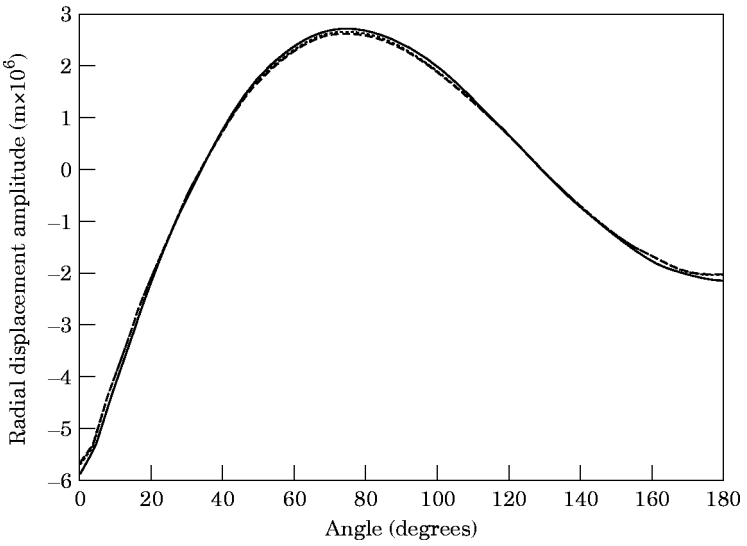

Figure 9. The radial displacements in the impedance and finite element models under dynamic out-of-phase loading at 5 Hz. ——, Impedance model; ----, FEM, with actuators; · · · · , FEM, without actuators.

amplitudes are shown in Figures 9 and 10 for out-of-phase and in-phase actuation, respectively. It can be observed that the impedance model matches the results of the finite element model without actuators. When the actuator stiffness is included, the displacements do not match the theoretical results. The discrepancies mainly occur in the actuator region, where the increased stiffness will reduce the radial displacement amplitude. Nevertheless, the results are comparable to those obtained by the impedance model.

At very low frequencies, the dynamic results should converge towards the static results. The static model for in-phase actuation developed by Lalande *et al*. [9] is also shown in

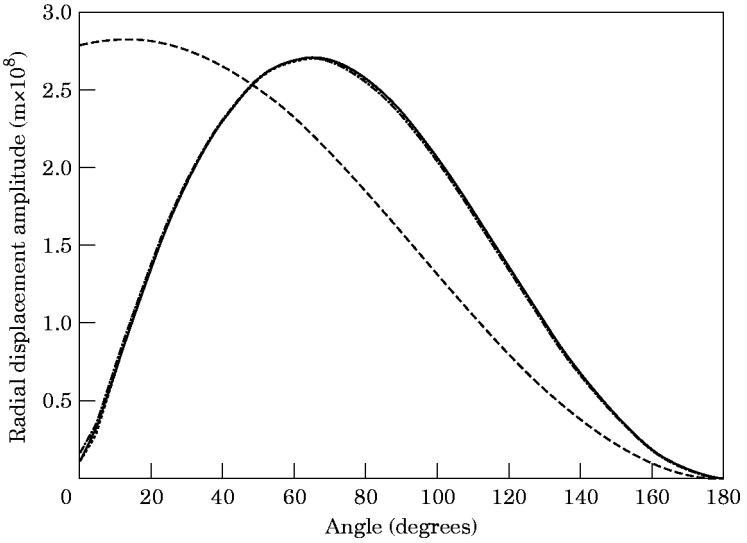

Figure 10. The radial displacements in the impedance, static and finite element models under dynamic in-phase loading at 5 Hz. ——, Impedance model, ----, FEM, with actuators; · · · · , FEM, without actuators; -·-·-·, static model.

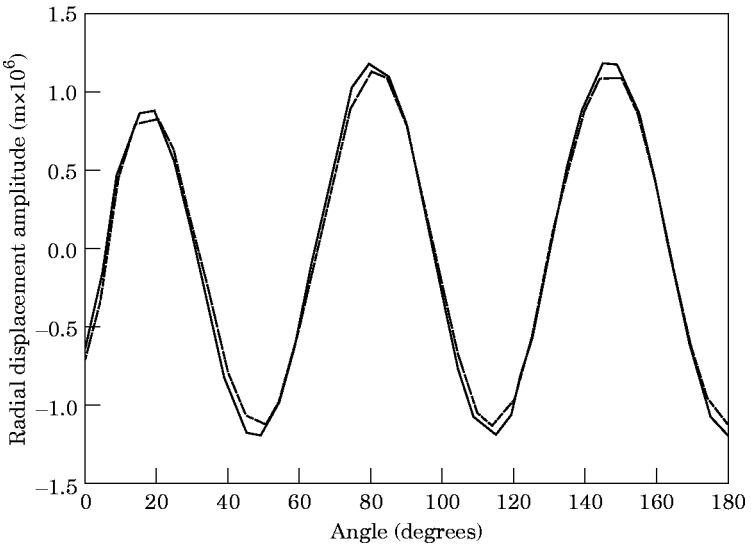

Figure 11. The radial displacements in the impedance and finite element models under dynamic out-of-phase loading at 450 Hz. ——, Impedance model; ----, FEM, with actuators; · · · ·, FEM, without actuators.

Figure 10. It can be seen that the displacement based on the static model matches the displacements based on the impedance model. A co-ordinate transformation, from free floating to fixed at 180°, was applied to the impedance and finite element models so that it could be compared with the static model.

The structural radial displacements at 450 Hz for out-of-phase and in-phase actuation, where the fourth mode is dominant, are shown in Figures 11 and 12, respectively. Once again, the displacements predicted by the impedance model match those obtained with the finite element model without actuators. If the actuator stiffness and mass are included, the

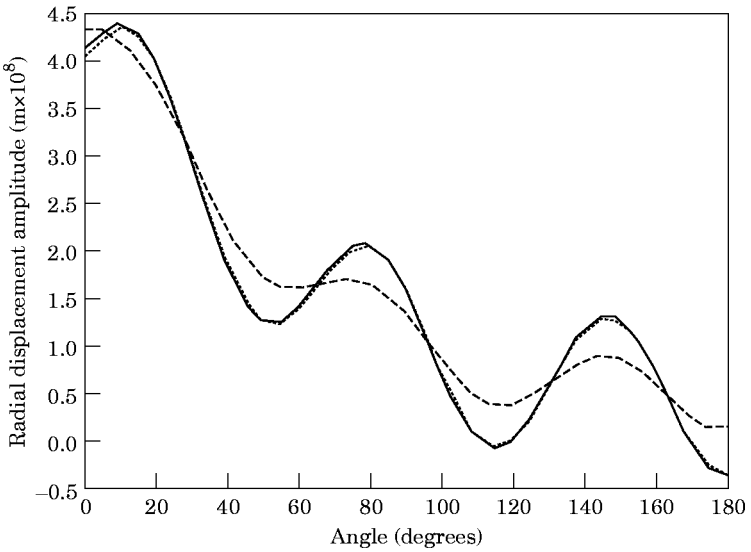

Figure 12. The radial displacements in the impedance and finite element models under dynamic in-phase loading at 450 Hz. ——, Impedance model; ----, FEM, with actuators; · · · ·, FEM, without actuators.

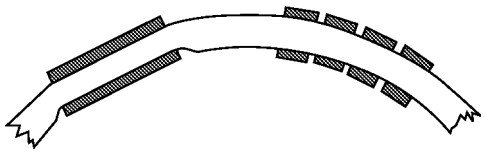

Figure 13. Methods for bonding flat actuators on curved structures.

displacements are slightly different, but still close enough for the theoretical model to be conclusive.

7. EXPERIMENTAL VERIFICATION

A steel ring actuated in-phase and out-of-phase by surface-bonded PZT actuators was to verify experimentally the impedance models. Before presenting the experimental apparatus and the experimental results, a discussion of the bonding of piezoceramic actuators on curved surfaces is presented.

7.1. BONDING OF PIEZOCERAMIC ACTUATORS ON CURVED SURFACES

Due to their brittle nature, piezoceramic materials can only tolerate a very small curvature before they will break. This creates a problem when actuators need to be used with curved structures. A possible way to obtain a curved piezoceramic actuator is to machine the desired curvature in a thick actuator. This method involves high machining accuracy, only provides limited curvatures and is expensive. It is also possible directly to fabricate actuators with a curvature, but this is also expensive. Thus, there is a need to adapt flat piezoceramic actuators to curved structures.

The most convenient way to apply an actuator on a curved structure is to machine a flat surface on the structure (Figure 13). This provides an easy and inexpensive means of obtaining the desired actuation/sensing. However, this technique is not possible for all situations. For large radius:thickness ratios, the matching of the flat surface can be done without affecting the structural properties of the shell; but for thin shells, the structural properties can be greatly modified. Also, the machining of a flat surface can be simply impossible due to the location or the size of the actuator/sensor.

An alternative to bonding flat piezoceramic actuators is to cut them into small pieces, and bond them next to each other on the structure (Figure 13). The piezoelectric pieces are bonded as closely as possible, but leaving a gap to avoid any electrical short-circuit. The space between the actuators is small enough to be neglected, so that all pieces can be considered as a single actuator. With a sufficient number of pieces, the actuator could be considered to be curved. This technique does not involve the machining of the structure and places no limits on the size of the actuator, but has other drawbacks. The first difficulty is the bonding of the actuators itself on the curved surface. For each piece, a non-uniform adhesive layer must be present to accommodate the flatness (Figure 14). Because of this,

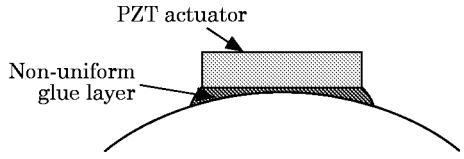

Figure 14. A schematic illustration of a non-uniform adhesive layer accommodating a flat PZT on a curved structure.

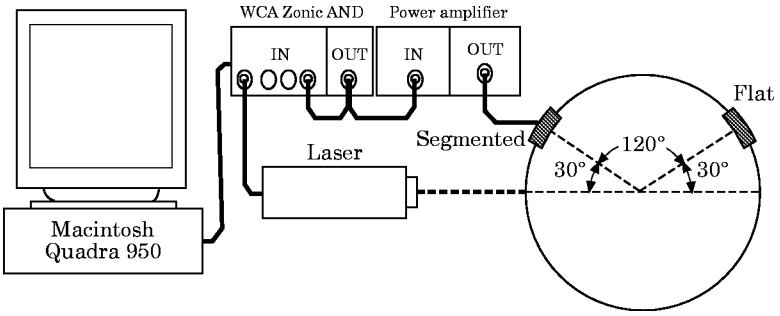

Figure 15. The experimental set-up used to measure the out-of-plane velocities of the structure.

it is very difficult to obtain bonding comparable to a flat actuator on a flat surface that will transfer the actuator's induced strain to the structure. A second difficulty is to bond each piece as close as possible to the next one, in order to obtain a global uniform patch, but leaving a gap for the electrical insulation. In this technique, it is assumed that each actuator piece will cancel the effect of the adjacent actuator, only producing a global effect on the structure.

7.2. EXPERIMENTAL APPARATUS

A random signal produced by the WCA Zonic and amplified with a Trek 50/750 high voltage power amplifier was applied to the piezoelectric actuators. The ring velocity response was measured using a Polytec laser vibrometer system and data was acquired with WCA Zeta software on a Macintosh Quadra. The experimental set-up is shown in Figure 15. The ring was suspended using fishing line to simulate free-floating boundary conditions. Finally, the out-of-plane velocity measurements were carried out at angles of 30° and 150° from the actuator. The laser vibrometer system is able to measure accurately velocities up to 1 μm/s. The experimental ring was chosen such that the velocities produced by the actuators, which are driven at half of the depoling electrical field, will be large enough to be measured accurately. The two bonding techniques discussed previously were used. First, a flat surface was machined on the ring. The structural integrity was not affected by the machining process due to the relatively large thickness and radius of the ring and the small actuator patch. Second, the actuators were bonded on the curved surface, breaking it into four pieces of 9 mm each and leaving a thin gap between each piece. For the remainder of the paper, the single piece continuous actuators bonded on the machined flat surface will be referred to as "flat actuators", while the segmented actuators bonded on the curved surface will be referred to as "segmented actuators".

7.3. EXPERIMENTAL RESULTS

The ring's radial frequency response at 30° from the actuator subjected to out-of-phase actuation is shown in Figure 16. The flat actuators show a better match to the impedance model than the segmented actuators. The segmented actuators produce smaller displacements than the flat actuators, due to the increased bonding layer thickness and gaps between each piece, which will reduce the actuators' authority on the structure. Nevertheless, both the flat and segmented actuators show a conclusive match with the theoretical impedance model.

The ring's frequency response at the same location due to in-phase actuation is shown in Figure 17. In this case, the match between the impedance model and the experimental results is not as conclusive. The differences might be attributed to the actual bonding of

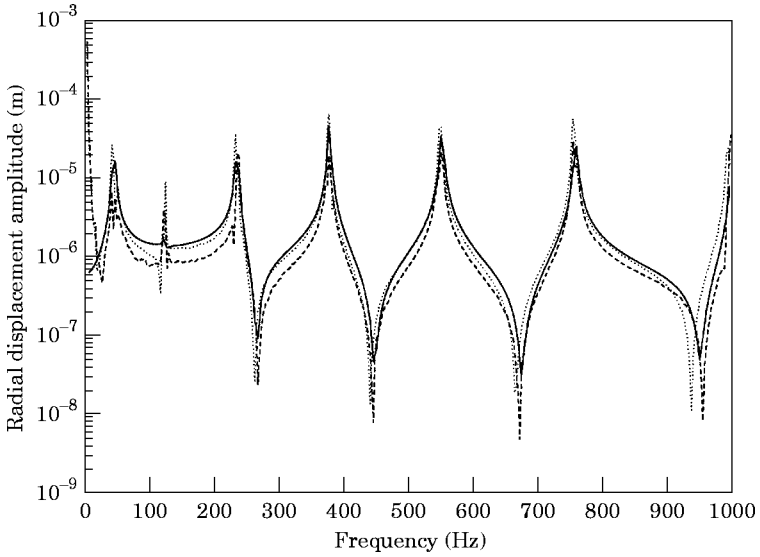

Figure 16. The experimental and impedance model ring response to out-of-phase actuation. ——, Impedance model; ----, experimental segmented actuators; · · · · , experimental flat actuators.

the actuators on the curved surface. The theoretical model cannot exactly model the actual experimental set-up, the bonding layer having an impact on the structural response, and likewise for the machined flat surface. Taking account of those considerations, the theoretical and experimental results show a good match at the resonant frequencies. The structural responses at 150° from the actuator are not presented, since the same conclusions would be drawn.

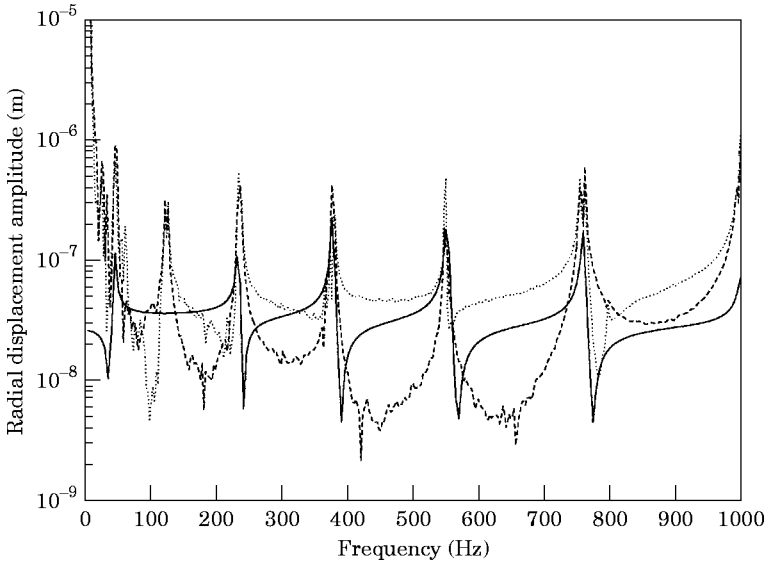

Figure 17. Experimental and impedance model ring response to in-phase actuation. ——, Impedance model; ----, experimental segmented actuators; · · · · , experimental flat actuators.

8. CONCLUSIONS

An impedance model for the actuation of induced strain actuators bonded to the surface of a circular ring has been developed. A discussion of the appropriate representation of the induced strain loading has shown that the actuation loading can be included either as induced uniform forces on the actuator footprint or as external equivalent loading. A comparison of the authority of in-phase and out-of-phase actuation of thin rings was performed. Based on the radial response of the ring, it is shown that in-phase actuation has lesser authority on the ring than out-of-phase actuation. Also, out-of-phase actuation is more efficient in exciting the lower order bending modes of the ring, while in-phase actuation has the capability of exciting the higher circumferential modes. The analytical results were verified using a dynamic finite element analysis with piezoelectric elements available in ANSYS 5.0. A good correlation between the impedance model and the finite element results validated the analytical model.

The experimental verification of the out-of-phase impedance model was very conclusive. An excellent match between the theoretical and experimental results was observed. However, the match is more difficult for the in-phase actuation case. Greater discrepancies are found due to the smaller displacements involved and to the greater sensitivity to the bonding of the actuators on the structure. Nevertheless, the in-phase actuation experimental results are still similar to the theoretical results, both in shape and magnitude.

ACKNOWLEDGMENT

The authors would like to acknowledge the funding support of the National Science Foundation through Grant #MSS-9157080 (Dr Ken Chong, Program Manager).

REFERENCES

1. E. F. Crawley and E. H. Anderson 1990 *Journal of Intelligent Materials Systems and Structures* **1**, 4–25. Detailed models of piezoceramic actuation of beams.
2. E. F. Crawley and J. de Luis 1987 *American Institute of Aeronautics and Astronautics Journal* **25**, 1373–1385. Use of piezoelectric actuators as elements of intelligent structures.
3. E. K. Dimitriadis, C. R. Fuller and C. A. Rogers 1991 *Journal of Vibration and Acoustics* **113**, 100–107. Piezoelectric actuators for distributed vibration excitation of thin plates.
4. B. T. Wang and C. A. Rogers 1991 *Journal of Intelligent Materials Systems and Structures* **2**, 38–58. Modeling of finite length spatially distributed induced strain actuators for laminate beams and plates.
5. E. F. Crawley and K. B. Lazarus 1989 *American Institute of Aeronautics and Astronautics Journal* **29**, 944–951. Induced strain actuation of isotropic and anisotropic plate.
6. N. W. Hagood, E. F. Crawley, J. de Luis and E. H. Anderson 1988 *American Control Conference*, *Atlanta*, *GA*, 1890–1896. Development of integrated components for control of intelligent structures.
7. H. C. Lester and S. Lefebvre 1991 *Recent Advances in Active Noise and Vibration Control*, *Blacksburg*, *VA* **3**, 3–26. Piezoelectric actuator models for active vibration control of cylinders.
8. V. R. Sonti and J. D. Jones 1991 *Recent Advances in Active Noise and Vibration Control*, *Blacksburg*, *VA*, 27–38. Active vibration control of thin cylindrical shells using piezo-electric actuators.
9. F. Lalande, Z. Chaudhry and C. A. Rogers 1994 *AIAA/ASME/ASCE/AHS/ASC* 35*th Structures*, *Structural Dynamics and Materials Conference*, *Adaptive Structures Forum*, *Hilton Head*, *SC*, 429–437. Modeling considerations for in-phase actuation of actuators bonded to shell structures.
10. P. H. Larson and J. R. Vinson 1993 *ASME Winter Annual Meeting Adaptive Structures Symposium*, *New Orleans*, *LA* AD-**35**, 277–285. The use of piezoelectric materials in curved beams and rings.

11. V. R. Sonti and J. D. Jones 1993 *Meeting of the Acoustical Society of America*, *Ottawa*, *Canada*. Curved piezo-actuator models for active vibration control of cylindrical shells.
12. C. Liang, F. P. Sun and C. A. Rogers 1993 *SPIE Conference on Smart Structures and Materials*, *Albuquerque*, *NM* **1917**, 286–298. Dynamic output characteristics of piezoceramic actuators.
13. S. Zhou, C. Liang and C. A. Rogers 1994 *SPIE Conference on Smart Structures and Materials*, *Orlando*, *FL* **2190**, 550–562. A dynamic model of a piezoelectric actuator driven thin plate.
14. A. Rossi, C. Liang and C. A. Rogers 1993 *AIAA/ASME/ASCE/AHS/ASC* 34*th Structures*, *Structural Dynamics and Materials Conference*, *La Jolla*, *CA*, 3618–3624. Impedance modeling of piezoelectric actuator-driven systems: an application to cylindrical ring structures.
15. S. Zhou, C. Liang and C. A. Rogers 1993 *ASME Winter Annual Meeting*, *Adaptive Structures Symposium*, *New Orleans*, *LA* AD-**35**, 247–255. Impedance modeling of two dimensional piezoelectric actuators bonded on a cylinder.
16. Z. Chaudhry, F. Lalande and C. A. Rogers 1994 *SPIE Conference on Smart Structures and Materials*, *Orlando*, *FL* **2190**, 563–570. Modeling of induced strain actuator patches.
17. W. Soedel 1976 *Journal of Sound and Vibration* **48**, 179–188. Shells and plates loaded by dynamic moments with special attention to rotating point moments.
18. F. Lalande, Z. Chaudhry and C. A. Rogers 1995 *SPIE Conference on Smart Structures and Materials*, *San Diego*, *CA* **2443**, 396–408. Impedance modeling of actuators bonded on shell structures.
19. A. W. Leissa 1973 *Vibrations of Shells*. *NASA SP*-288. Washington, D.C.: U.S. Government Printing Office.
20. W. Soedel 1981 *Vibrations of Plates and Shells*. New York: Marcel Decker.
21. L. Meirovitch 1986 *Elements of Vibration Analysis*. New York: McGraw-Hill.